https://ntrs.nasa.gov/search.jsp?R=19850027030 2020-03-20T17:13:36+00:00Z

NASA Contractor Report 178045

ADVANCED DETECTORS AND SIGNAL PROCESSING

D. W. Greve, P. H. L. Rasky, and M. H. Kryder

CARNEGIE-MELLON UNIVERSITY
Pittsburgh, Pennsylvania

Grant NAG1-395
February 1986

(NASA-CR-178045) ADVANCED DETECTORS AND SIGNAL PROCESSING Final Report (Carnegie-Mellon Univ.) 28 p HC A03/MF A01 CSCL 09C

N85-35343

Unclas
G3/33 27507

National Aeronautics and
Space Administration

Langley Research Center
Hampton, Virginia 23665

Advanced Detectors and Signal Processing*

D.W. Greve, P.H.L. Rasky, and M.H. Kryder

Abstract

We report continued progress toward development of a silicon- on-garnet technology which would allow fabrication of advanced detection and signal processing circuits on bubble memories. The first integrated detectors and propagation patterns have been designed and incorporated on a new mask set. In addition, annealing studies on spacer layers have been performed. Based on those studies, we proposed a new double layer spacer which should reduce contamination of the silicon originating in the substrate. Finally, we have measured the magnetic sensitivity of uncontaminated detectors from our last lot of wafers. The measured sensitivity was lower than anticipated but still higher than present magnetoresistive detectors.

* Supported by National Aeronautics and Space Administration Grant NAG-1-395.

I. Introduction

In this report we summarize the work performed in the preceding year under the contract "Advanced Detectors and Signal Processing for Bubble Memories." In the preceding contract period, we had successfully fabricated operating semiconductor devices on bubble substrates. We report here further development of the silicon- on- garnet technology and progress toward integration of detectors and bubble propagation patterns.

The following section presents a brief summary of the characteristics of semiconductor detector structures for magnetic fields. In Section III, we then describe how two of these detector types can be integrated with bubble propagation patterns. Section IV reports on studies of new types of spacer layers which are intended to reduce contamination problems we have experienced. In Section V, we describe the performance of magnetic detector structures fabricated on silicon wafers which should be similar to detectors made on bubble substrates with an improved spacer layer. Finally, in Section VI we describe our plans for further work in this area.

II. Physics of Magnetic Detectors

In this section, we discuss the characteristics of various types of semiconductor detectors of magnetic fields. The emphasis will be on the suitability of these detectors for our silicon- on- garnet technology. A more complete discussion of magnetic detectors is available [1].

The earliest and most obvious semiconductor detector is the conventional Hall plate shown in Fig. 1. Indeed, any conducting material can be used to make a Hall plate but semiconductors are best since we have [2]

$$V_H = \mu_n \xi B d$$

where V_H is the Hall voltage, ξ the electric field applied to the sample, and d is the width. Higher sensitivity is therefore obtained in materials with high mobility μ_n.

The motivation for more complex structures is the potential for higher sensitivity. This higher sensistivity may result from intrinsic amplfication present in the detector structure or from the exploitation of surface effects. We consider first detector structures which work by current steering between electrodes of an amplifying device. We will then discuss detectors which utilize surface effects to obtain high sensitivity.

Figure 2 shows a two- collector bipolar transistor suitable for use as a magnetic field detector. The highest reported sensitivities (as large as 13 V/T) have been for magnetic field detectors of this type [3]. In principle, this detector could be fabricated in recrystallized polysilicon; in this case one would expect from the geometry that it would be sensitive primarily to normal magnetic fields. However, bipolar transistors in recrystallized polysilicon films have not had good performance [4].

Multiple drain field effect transistor detectors seem more promising since good field effect mobilities are observed in recrystallized material (in contrast to the poor minority carrier lifetimes). Figure 3 shows a detector with three drains [5]. The Hall probes are connected to a biasing potential through two load resistors. In this case the operation is as if the drain current was deflected by the magnetic field. From the geometry, we expect sensitivity primarily to normal fields. Better sensitivity is obtained in the voltage mode with a measured sensitivity of up to 2 V/T [5] when the device is operated in the pinched off mode. This type of detector fits very well into our technology since the bubble can be propagated beneath the detector. However, photolithographic limitations make it necessary to build detectors considerably larger than the bubble diameter. We expect the sensitivity to be degraded by a factor of order d/w, where d is the bubble diameter and w is the channel width.

For completeness, it is worth mentioning the carrier domain magnetometers [6]. These devices (not illustrated) are bipolar transitors with multiple collectors placed symmetrically around an emitter. The output is a frequency proportional to the applied magnetic field. These devices are not easily adaptable to our technology where detection of a magnetic bubble is the goal.

Finally, we consider magnetodiodes as illustrated in Fig. 4. Magnetic

fields in the direction shown in the figure tend to deflect carriers either toward or away from the bottom interface. In SOI technologies the top and bottom interfaces have different surface recombination velocities so one observes a change in device voltage for constant current. Best results are obtained when a double injection filament forms with sensitivities as high as 10 V/T [7]. We note that this structure is sensitive to fields parallel to the surface of the wafer.

From the above, it is clear that only magnetodiodes and multiple drain field effect transistors are good prospects for use in a silicon- on- garnet technology. These two detector types will require different designs since they are sensitive to different components of the bubble's magnetic field. In the following section, we will indicate how we can integrate each of these detector types with magnetic bubble propagation patterns.

III. Design of integrated detectors and propagation patterns

A major objective of our work is to demonstrate integration of silicon bubble detectors with propagation patterns. We therefore devoted some of our time to design of a mask set which would allow us to fabricate both silicon devices and propagation patterns on the same chip. Previously, we had fabricated silicon devices only and we studied the magnetic properties using magnetooptic techniques [8].

Figure 5 shows an overall view of our second silicon-on-garnet mask set. There are seven mask levels. In Fig. 6, we illustrate the process steps necessary to fabricate a field effect transistor near a bubble propagation track. After deposition of the spacer layer, polysilicon is deposited, recrystallized, and islands are defined with the first mask level. After growth of a thin protection SiO_2 layer, the n+ and p regions are defined with photoresist masking. The p region is defined with the second mask level and the n+ region with level three. In this structure, the p+ mask (level four) is not used. We then grow the gate oxide and cut contact windows with mask level five and define the aluminum metallization with level six. Finally, level seven is used to mask the hydrogen implantation which defines ion-implanted contiguous-disk bubble propagation patterns.

The mask also contains an assortment of test structures which will allow us to characterize the process and verify that all structures are operating. The test structures include resistors, MOS capacitors, diodes and MOSFETs. Included on the mask set are the two most promising silicon- on-garnet detectors: multi-drain field effect transistors and magnetodiodes. In addition to isolated detectors for sensitivity studies; some detectors are integrated with bubble propagation patterns. We will then be able to use silicon devices to sense magnetic bubble domains. We will now discuss in detail the design and operation of these novel structures.

We first discuss the multi-drain field effect transistor structures. Figure 7 shows a top view of such a detector; a cross section is shown in Fig. 6d. The bubble propagation pattern is also shown beneath the detector. Our design is essentially a scaled down version of Fry's three drain MAGFET [5]. We place the propagation pattern underneath the gate so that the detector effectively senses the perpendicular component of the bubble's fringing field. The propagation pattern is formed by ion implantation with hydrogen, deuterium, or helium before the aluminum deposition and patterning. The implantation energy is chosen so that the ions come to rest in the epitaxial film. If the dose is large enough a thin in-plane drive layer will result [9]. The 0.2- 0.5 μm thick silicon film is relatively transparent to the implanted species [10]. Even so, some of the hydrogen will come to rest in the silicon film. However, recent work has shown that this hydrogen will have a beneficial effect on the transistor characteristics [11].

Since our detectors are smaller than those previously reported it is possible that the sensitivity will be different. We can use first order Hall effect theory to estimate the change in sensitivity. For an ordinary Hall plate, the Hall voltage is

$$V_H = BJd/\rho$$

where B is the applied magnetic field, J is the current density, d is the separation of the Hall probes, and ρ is the charge density in the semiconductor [12]. Strictly speaking, this equation gives the output voltage for a uniformly doped Hall plate under open circuit conditions; we

assume that it also gives the correct dependence of output voltage on device dimensions for a silicon- on- garnet MAGFET. For a constant current density J, we are led to expect a sensitivity 10-20 times smaller than Fry's since the separation between our Hall probes is 10-20 times smaller. Even though this is low (approximately 0.125 V/T), it is still sufficiently large to make detection of bubble domains feasible. In fact this estimate suggests that signals comparable to those from presently manufactured bubble devices in which the bubble is stretched to 100 times its normal diameter could be obtained from a single unstretched bubble. We note that this estimate is somewhat uncertain since it is not clear what the appropriate value of ρ would be.

We now consider the magnetodiode detectors. The high sensitivity of magnetodiodes, with 5- 80 V/T values reported [13,14], makes this device a natural candidate for bubble detectors. Figure 8 shows our design for a magnetodiode detector. Magnetic bubbles move along the bubble propagation pattern in the usual way until they reach the hairpin stretcher. The hairpin stretcher is activated by applying a large current pulse of 100- 200 mA, causing the effective bias field in the ion- implanted channel to be lowered. If a bubble is present when this occurs, the bubble will expand into the channel. The in- plane component of the bubble's magnetic field is then sensed by the nearby magnetodiode.

It is difficult to make an estimate of the effectiveness of this detector. Since it detects the in- plane component, the signal produced by a bubble is expected to be a strong function of the separation between the detector and the ion- implanted channel and also the thickness of the spacer layer. However, because of the use of the stretcher, we expect the sensitivity to be higher than the MAGFET. The stretcher field is also sensed by the diodes, however, so it is necessary to operate this detector in a differential mode with a dummy sensor as shown in Fig. 9.

IV. Process development

Our previous work showed that the field effect transistors fabricated on garnet had considerably higher gate leakage and lower channel mobility

the film thickness was less than 2000 Å. Thicker films cracked and peeled, probably as a consequence of the very high tensile stress of Si_3N_4 [17]. The film uniformity with this process was not good (thickness variations of ± 20% across a wafer) but this can be improved somewhat with better boat design [18].

When silicon nitride was deposited on bubble wafers with this process, we observed blackening of the bubble film. Silicon wafers which were deposited in the same run did not show this blackening. We therefore suspected decomposition of the magnetic epitaxial layer during the deposition. Some bubble film compositions are stable when heated in either oxygen or nitrogen at this temperature [8]. We therefore suspected hydrogen or ammonia was responsible for the decomposition.

We chose to test the stability of bubble films exposed to ammonia alone at this temperature. We annealed a magnetic bubble film with composition $Y_{0.8}Sm_{0.3}Tm_{1.3}Gd_{0.6}Fe_{4.6}Al_{0.2}Ga_{0.2}O_{12}$ in a NH_3 ambient at 800 °C with a pressure of 0.68 Torr. This produced a grayish haze on the surface of the bubble substrate. SEM micrographs showed that the haze was a continuous film composed of a network of interdigitated rod- like objects. The rods were approximately 700 Å in diameter and are at least a micrometer long.

In order to further characterize the chemistry of the haze we used scanning Auger analysis. Figure 10 shows the Auger spectra observed after different sputtering times. At the top of the figure we show the surface of the film; Fe and O are readily detected but other components of the bubble film like Sm, Gd, Y, and Tm are absent. Going deeper (second and third traces) we observe Sm, Gd, Y, and Tm in addition to Fe. The Auger data suggests that the primary mechanism for formation of the haze is diffusion of iron to the surface fo the epitaxial film. It is clear that exposure to NH_3 at these temperatures is a problem. There may be additional damage due to the presence of hydrogen.

The experiment discussed above showed that silicon nitride cannot be deposited directly on a bubble substrate. We also examined the possibility of depositing silicon nitride on a protected bubble substrate. As a test, a

than transistors fabricated on silicon wafers [8]. We attributed these problems to contamination of the silicon film and the gate oxide by metallic ions from the bubble film. This conclusion was supported not only by comparison of field effect transistors made on different substrates but also by the observation of crystalline defects after high temperature annealing. We therefore have worked on further development of the process technology, with particular emphasis on substitutes for the sputtered SiO_2 spacer layer.

Materials suitable for use as a spacer layer include aluminum oxide and silicon nitride. Both of these are known to be barriers for some contaminants. We chose to use silicon nitride because of the availability of deposition equipment. We also had the possibility of different deposition techniques which require different maximum temperatures.

Silicon nitride has been commonly used as a diffusion barrier in silicon technology. Appels et al. [15] introduced the use of silicon nitride as an oxygen barrier in local oxidation processes. In addition, Dalton and Drobek showed that sodium seldom diffuses more than 50 Å into high quality silicon nitride films [16]. Since sodium is a very small ion, it seems likely that silicon nitride will also be an effective barrier for heavy metals.

In our first experiments, we used LPCVD (low pressure chemical vapor deposition) to deposit silicon nitride. The source gases of silane and ammonia undergo the reaction

$$3\,SiH_4 + 4\,NH_3 \longrightarrow Si_3N_4 + 12\,H_2 \ .$$

We deposited silicon nitride on both bubble wafers and silicon pilot wafers. The deposition was done at 800 °C and a pressure of 0.66 Torr; SiH_4 and NH_3 flow rates were 10 and 60 sccm, respectively. Wafer to wafer separation was 1 cm and the deposition rate was approximately 36 Å/min.

Depositions of silicon pilots gave films with good appearance provided

bubble film coated with 1 µm of sputtered SiO_2 was annealed in a NH_3 ambient under the same conditions used to anneal the uncoated bubble film. This time, however, we could not detect any visual signs of bubble film decomposition. This encouraging result indicates that it may be possible to use LPCVD nitride in a double layer structure. However, in order to make it more likely that we would get working devices in the next set of wafers, we chose to pursue a safer alternative.

Figure 11 shows the spacer structure which was used for the lot presently in process. We first deposit 4000 Å of sputtered SiO_2 followed by 3000 Å of plasma nitride. The plasma nitride deposition can be done at low temperatures (~35 °C) and is therefore less likely to cause damage to the bubble film. We then deposit 5000 Å of polysilicon as usual. Spacer layers of this type were deposited on both bubble and silicon substrates. Silicon substrates were included as process pilots. As in our previous work, comparison of devices made on the silicon pilots and our bubble wafers will allow us to determine the degree to which contamination occurs with this new spacer layer.

Wafers from this lot have been laser recrystallized and the next step in the process is ion implantation. Microscopic examination of wafers after polysilicon deposition showed indications of some localized defects, however. Figure 12 shows a scanning electron micrograph just after polysilicon deposition. It appears that one or more of the top layers have popped off during or after polysilicon deposition. The silicon pilots did not have any such defects. It appears that the layers on the bubble substrate were simply under more stress. It should be noted that the plasma nitride process is somewhat more susceptible to particulate contamination and pinholes than the LPCVD nitride process [19]. The problems we have had do not appear to be fundamental since stress problems can be reduced with optimization of the deposition process or thickness, and pinhole densities can be reduced with cleaner processing. We therefore expect to produce working devices with possibly better characteristics than our last set. Due to localized defects, however, yield will probably continue to be a problem.

V. Magnetic measurements on dual- drain FETs

In this section, we report measurements of one type of magnetic detector which we fabricated in our last set of wafers. The characteristics of the working devices on bubble substrates were comparitively poor. We therefore chose to measure detectors fabricated on silicon substrates. The measurements we report should be characteristic of detectors on bubble substrates in the absence of contamination from the substrate.

The structure of the dual-drain magnetotransistor we fabricated and characterized is shown in Fig. 13. Figure 13a shows the top view and Figs 13b and 13c show the cross sections corresponding to sections AB and CD, respectively. We also indicate in Fig. 13d the circuit symbol used to represent a dual-drain magnetotransistor. The 5000- 6000 Å thick recrystallized silicon layer is separated from the silicon substrate, which acts as a back gate, by a 1 µm thick thermal SiO_2 spacer layer. The aluminum gate is approximately 1 µm thick and the (front) gate oxide thickness is 0.1 µm. The gate width and the drain to drain separation are both 10 µm. Devices selected for detailed measurement were attached to a nonmagnetic paddle and connected to large contact pads by wire bonding. The magnetic field for measurements was produced by a rare earth cobalt permanent magnet which produced a field of 2300 gauss.

Our test methodology broke electrical characterization of the dual-drain device into two parts. We first used a Hewlett Packard 4145A Semiconductor Parameter Analyzer to check device functionality. A device was defined to be functional if MOSFET characteristics were observed between both sets of gate, source, and drain terminals. These functionality measurements were made with the back gate and unused drain terminal tied to ground potential. In principle, this makes the unused drain electrically inactive and hence allows treatment of the five terminal structure as a single MOSFET. Functional devices were then wire bonded and rechecked again after mounting.

The second phase of the characterization procedure was the

investigation of magnetic field sensitivity. We connected the magnetotransistor in the circuit of Fig. 14. The drain voltages V_{DD1} and V_{DD2} were selected so that the differential output voltage ΔV was zero to $\pm$ 0.5 mV with no applied magnetic field. In general, V_{DD1} was not equal to V_{DD2} due to asymmetry in the fabricated device. This was possibly due to misalignment and/or the random location of the grain boundaries. Characteristics of a typical dual- drain device are shown in Figure 15. The drain currents I_{D1} and I_{D2} are plotted using the same vertical axes which clearly reveals the asymmetry between the two drains.

To check the sensitivity of the detectors, we chose R_L = 10 KΩ, V_{GS} = 2.0 V, and V_{BG} = 0.0 V. In addition, ΔV was 1.7 V for V_{DD1} = 35 V and V_{DD2} = 0. For an ideal device in which both drains were independent, this would correspond to the value of V_{DS} during our magnetic measurements. Since we found later that there was leakage between the drains, we can only say that V_{DS} was of the order of 1.7 V. The nominal drain currents during the measurement was therefore about 3 mA.

With a 0.23 Tesla perpendicular magnetic field applied, we measured ΔV = 5 mV for one direction of the applied field and a similar change in the negative direction with the field reversed. We therefore calculate a sensitivity of .022 $\pm$ .002 V/Tesla. We note that the circuit parameters were not optimized and greater sensitivity may be observed after careful selection of the operating point.

Our measured sensitivity, 0.022 V/T, is an order of magnitude lower than the best value of 0.25 V/T observed by Fry and Hoey [5], but our results are still higher than a Hall detector. The results also represent the first successful demonstration of multi-drain field effect transistors in laser recrystallized silicon.

Improvements in device performance are likely if a three- drain configuration is used [5]. We also have evidence that a channel exists on the back surface of our devices which could degrade the sensitivity. This is

because a conducting path between the drains means that the Hall voltage sees a finite load resistance which always results in a lower output voltage.

We observed the existence of a back channel by measuring I-V characteristics between D1 and D2 for a number of gate and back gate voltages. Essentially, we treated one of the drains as the source of a field effect transistor; the actual source contact was tied to ground during these measurements. In all cases, it was found that a significant current flowed between the two drains; this current was on the order of 100-500 μA. However, the top and bottom gates did modulate the magnitude of this current; the current was smaller for more negative front or back gate voltages. This trend was observed for back gate voltages up to -10V. Making the back gate voltage even more negative resulted in increasing leakage current between the two drains. This anomalous result was a consequence of back gate oxide breakdown at an electric field of about 10 V/μm. This is two orders of magnitude less than is commonly reported [20] in the literature for thermal silicon dioxide. This low breakdown voltage is not surprising for the relatively poor oxides formed by sputtering.

A low back gate breakdown field is not a fundamental limitation assuming that one can turn off the back gate channel at lower voltages. McGreivy suggested a deep p+ ion implantation to produce a heavily doped region near the back surface of the silicon [21]. This increases the threshold voltage of the back channel and therefore suppresses the leakage current. We must, however, note that the back gate induced channel is not the only leakage mode possible. Drain to drain leakage current may also result if n-type impurities form conducting paths between the drains, by fast diffusion along grain boundaries. Minimizing this effect may require adjustments in the maximum process temperatures.

VI. Summary

In this period, we have designed and begun fabrication of a mask set which integrates magnetic detectors with bubble propagation patterns. Our designs were based on the detector physics which determines the field components to which the detector is sensitive. Because of this, different

designs are required for the magnetoresistive and field effect detectors.

We have also measured the sensitivity of detectors previously fabricated in recrystallized silicon on silicon substrates. The sensitivities were lower than expected, but this may be partly attributable to the existence of leakage between the two drain electrodes. In our next set of wafers, we expect to choose doping parameters and diffusion temperatures to minimize this effect.

Finally, we have examined the changes which occur to bubble films during LPCVD deposition of silicon nitride. Although some reaction appears to take place, the reaction can be minimized by first depositing a silicon dioxide layer. Plasma nitride also appears to be a promising alternative.

This study is expected to continue under other funding. Our major objectives in the near future will be the completion of a wafer set using the plasma nitride spacer layer and additional studies of annealing effects, particularly during LPCVD deposition.

References

1. "Integrated silicon multicollector magnetotransistors," V. Zieren, unpublished Ph.D. thesis, Technische Hogeschool Delft (1983).

2. "Physics," D. Halliday and R. Resnick, p. 828 (Wiley, 1962).

3. A.W. Vinal and N.A. Masnari, "Magnetic transistor behavior explained...," IEEE **EDL-3**, 203 (1982).

4. M. Rodder and D.A. Antoniadis, "Silicon- on- insulator bipolar transistors," Paper VB-4, Device Research Conference (1983).

5. P. W. Fry and S. J. Hoey, "A Silicon MOS Magnetic Field Transducer of High Sensitivity," IEEE **ED-16**, 35 (1969).

6. M.H. Manley and G.G. Bloodworth, "The carrier- comain magnetometer: a novel silicon magnetic field sensor," *Solid St. and Electron.Dev* **2**, 176 (1978).

7. A. Mohaghegh et al., "Double- injection phenomena under magnetic field in SOS films: A new generation of magnetosensitive microdevices," IEEE **ED-28**, 237 (1981).

8. P.H.L. Rasky et al, "Silicon- on- garnet MOSFETs..., NASA Report CR 172534, (1984).

9. A. H. Eschenfelder, "A Magnetic Bubble Technology," Springer-Verlag, 1981, p. 126.

10. J. F. Gibbons, W. S. Johnson, S. W. Mylroie, "Projected Range Statistics," 2nd edition Halsted Press, 1975.

11. H.J. Singh et al., "Hydrogenation by ion implantation for VLSI/SOI applications," Paper VB-2, Device Research Conference, Santa Barbara, CA (1984).

12. J. Millman, "Micro-Electronics," McGraw-Hill, 1979, p. 18.

13. O. S. Lutes, P. S. Nussbaum, O. S. Aadland, "Sensitivity Limits in SOS Magnetodiodes," IEEE **ED-27**, 2156 (1980).

14. G. A. Egiazaryan, G. A. Mantsakanyan, V. I. Murigin and V. I. Staveev, "Silicon Magnetodiodes Sensitive to Magnetic Field Direction," *Sov. Phys. - Semicond.*, **9**, 829 (1975).

15. J.A. Appels et al., "Local oxidation of silicon and its application in semiconductor technology," *Philips Res. Rep.*, **25**, 118 (1970).

16. J. V. Dalton and J. Drobek, "Structure and Sodium Migration in Silicon Nitride Films," *J. Electrochem. Soc.* **115**, 865 (1968).

17. "VLSI Technology," edited by S. M. Sze, McGraw-Hill 1983, p. 120.

18. R. Howe (MIT), private communication.

19. T. Tamagawa (Yale University), private communication.

20. A.S. Grove, "Physics and Technology of Semiconductor Devices," p. 103, (Wiley, 1967).

21. D.J. McGreivy, "On the origin of leakage currents in silicon- on-sapphire MOS transistors," IEEE **ED-24**, 730 (1977).

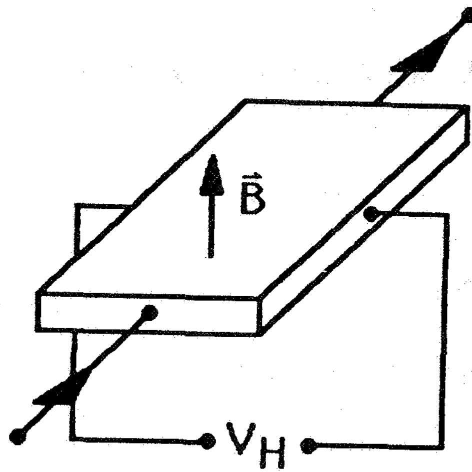

Figure 1: Conventional Hall plate.

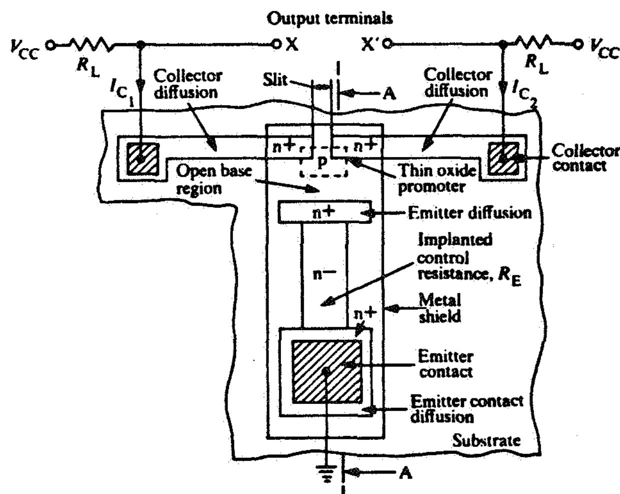

Figure 2: Two-collector bipolar transistor sensitive to perpendicular magnetic fields [3].

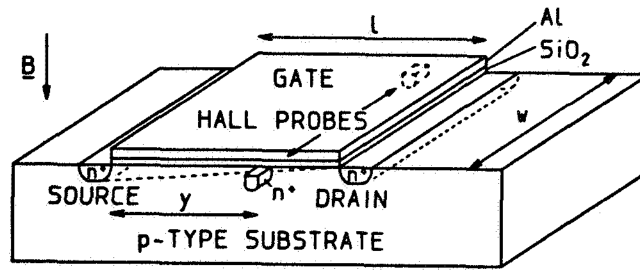

Figure 3: Multi-drain field effect transistor sensitive to perpendicular magnetic fields.

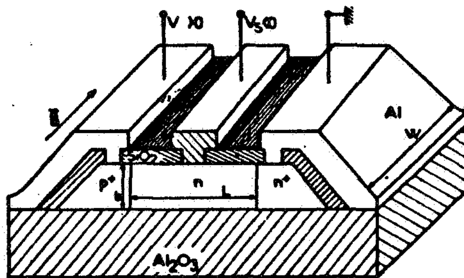

Figure 4: Magnetodiode as reported by Mohaghegh et al. [7].

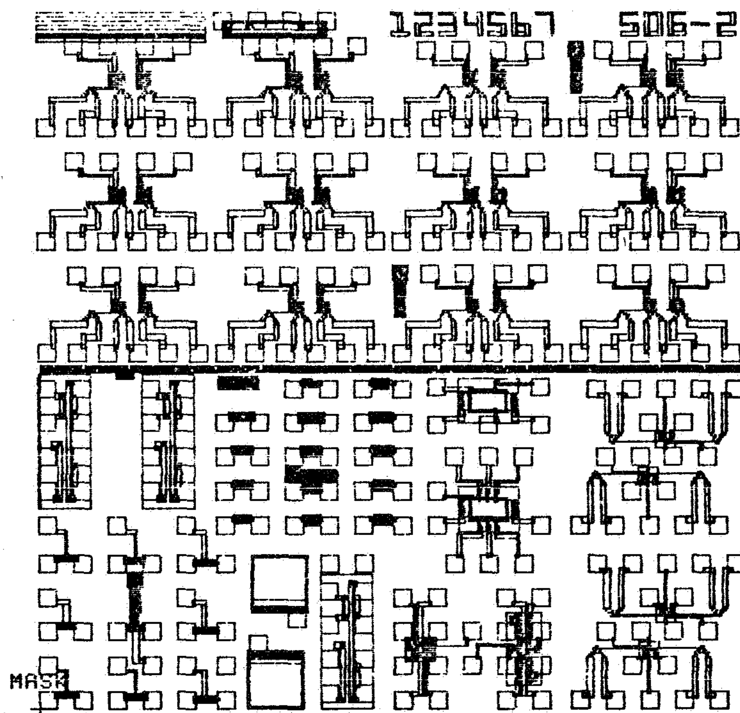

Figure 5: Seven layer composite plot of the second silicon- on- garnet mask set.

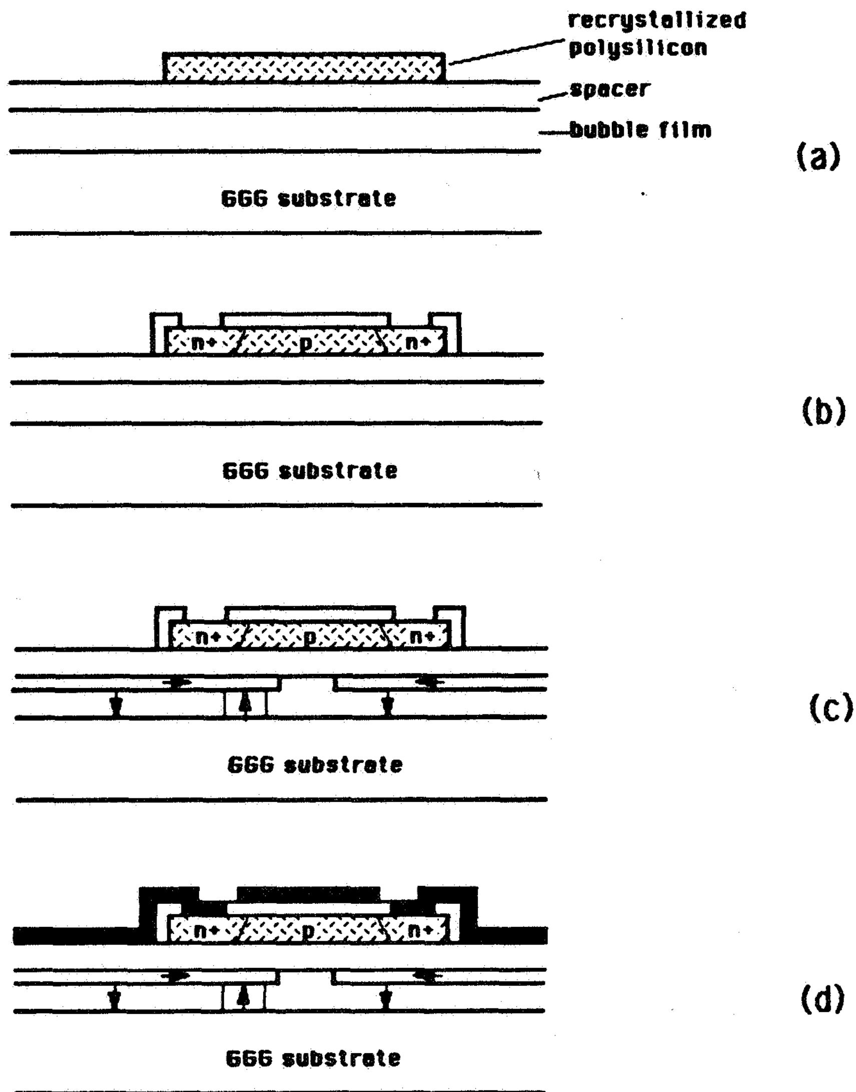

Figure 6: Silicon-on-garnet cross sections after various process steps for a MOS device.

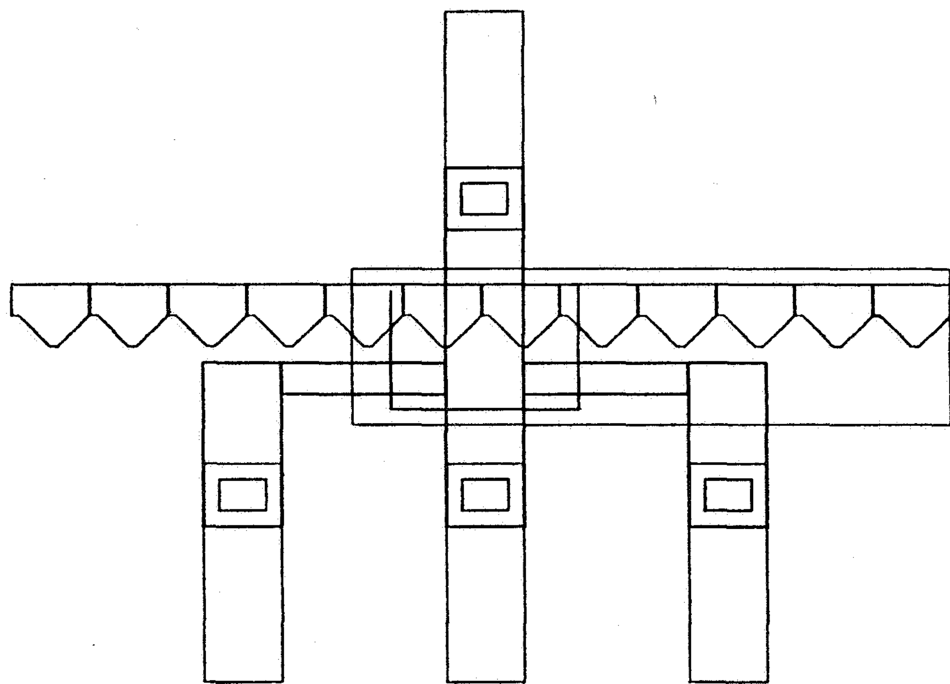

Figure 7: Top view of a three drain field effect transistor.

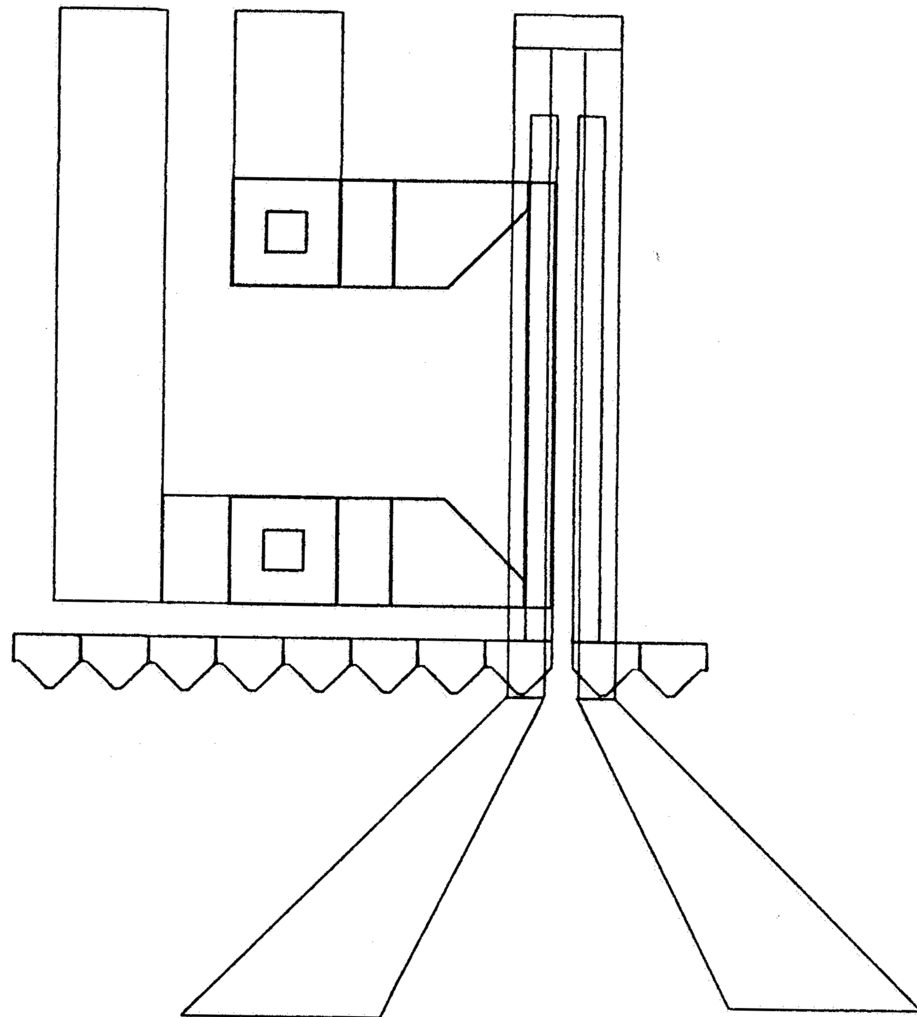

Figure 8: Top view of a silicon- on- garnet magnetodiode with integrated bubble propagation pattern.

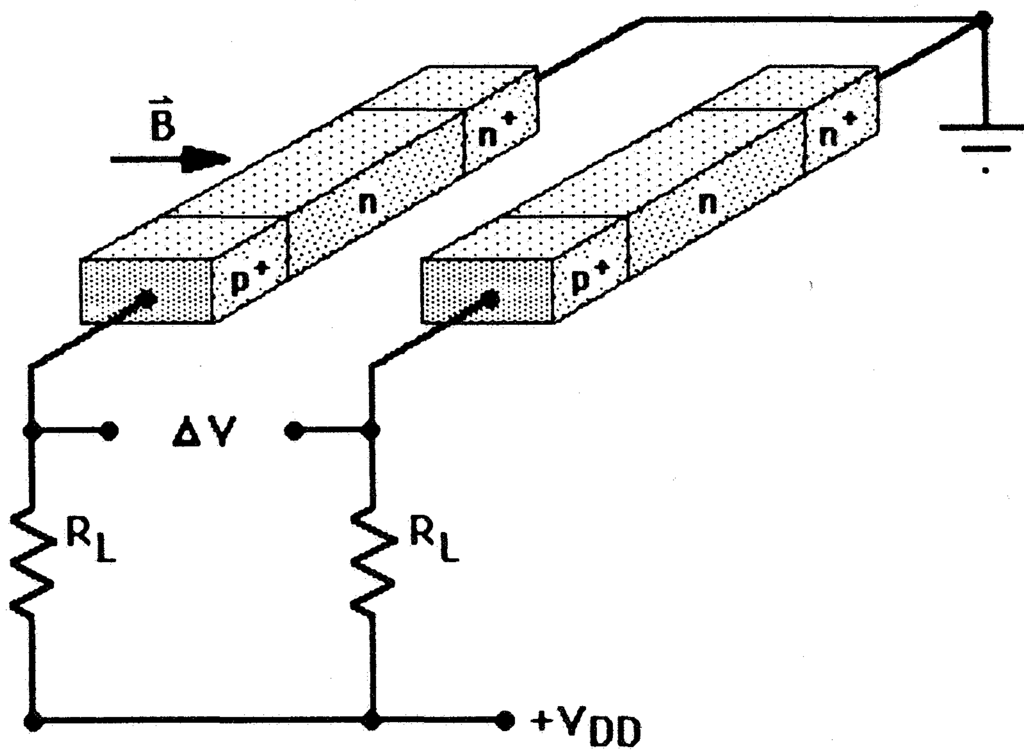

Figure 9: Magnetodiodes connected in a differential detection circuit.

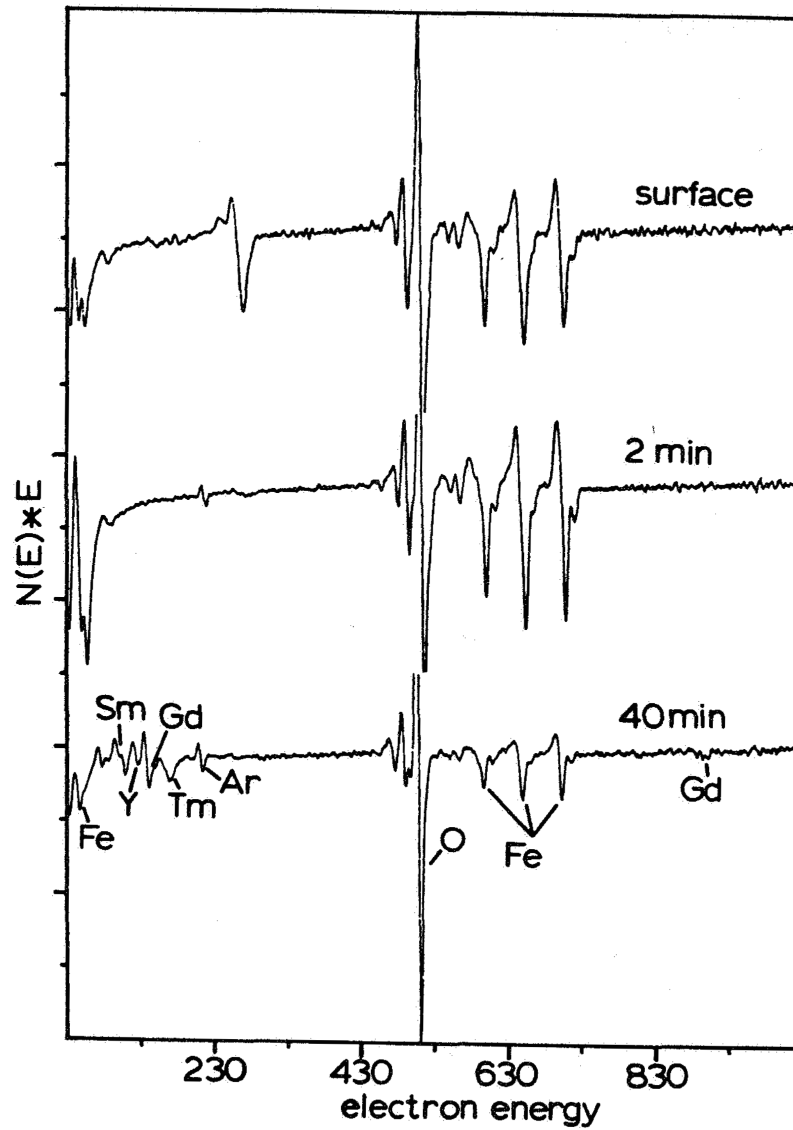

Figure 10: Auger spectra of the NH_3 induced haze for sputtering times of 0, 2, and 40 min.

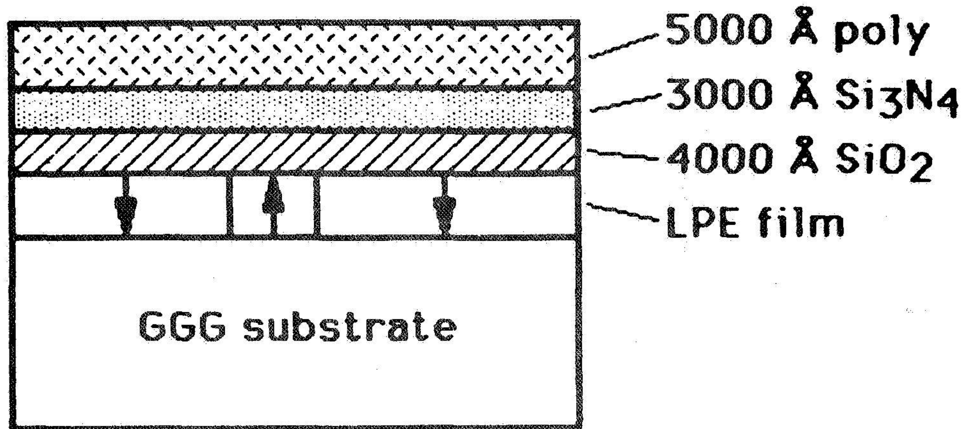

Figure 11: Cross section showing the double layer spacer structure used in the second silicon- on- garnet lot.

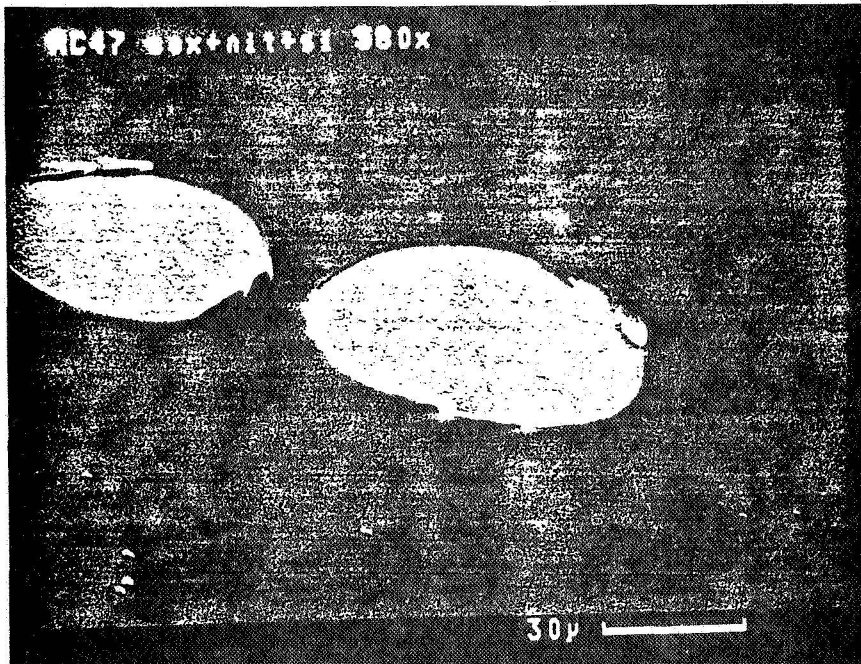

Figure 12: SEM micrograph of disk shaped defects observed in double layer spacer structures coated with polysilicon.

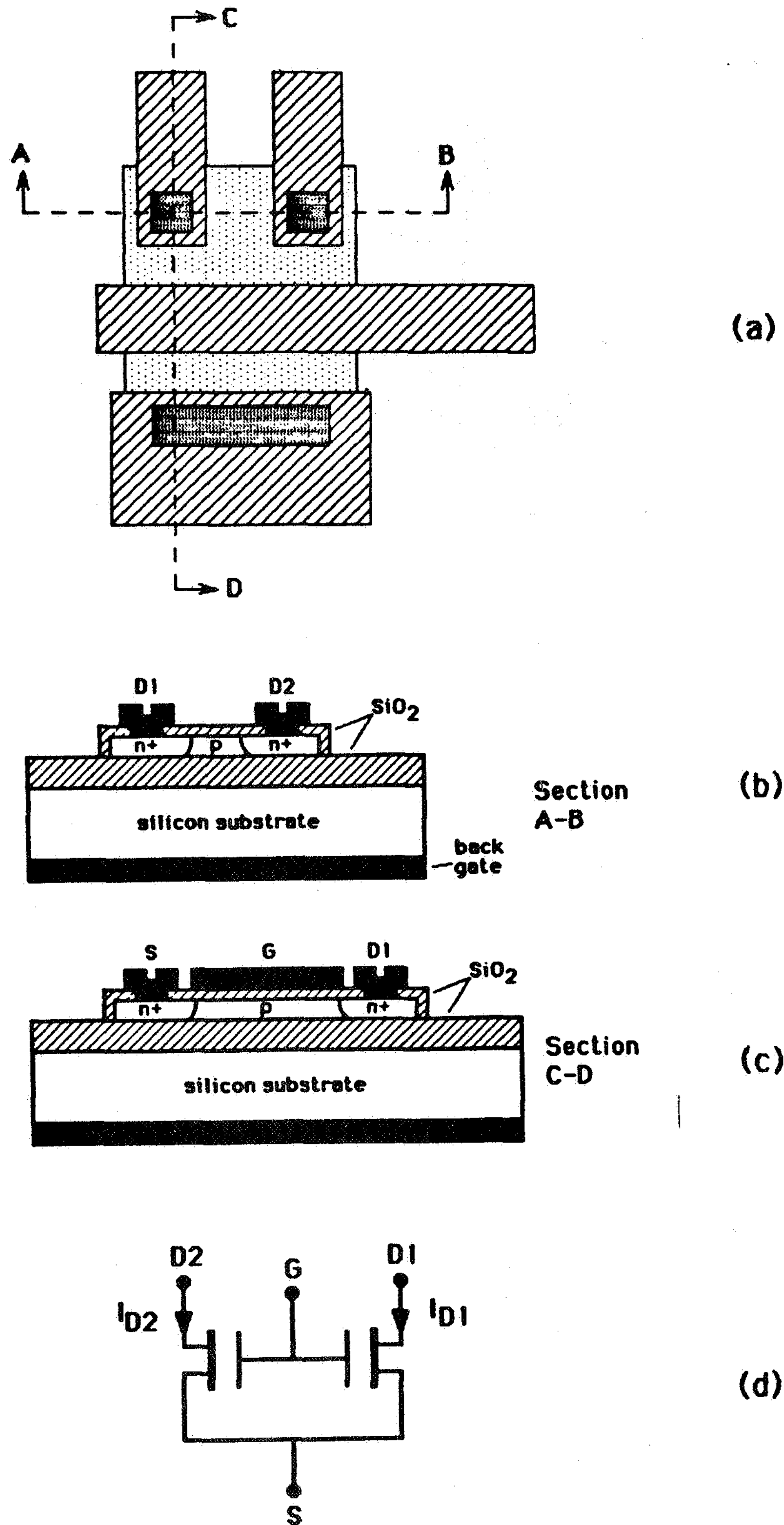

Figure 13: Dual drain MAGFET: (a) top view; (b),(c): cross sections along directions indicated in the top view and (d) circuit symbol.

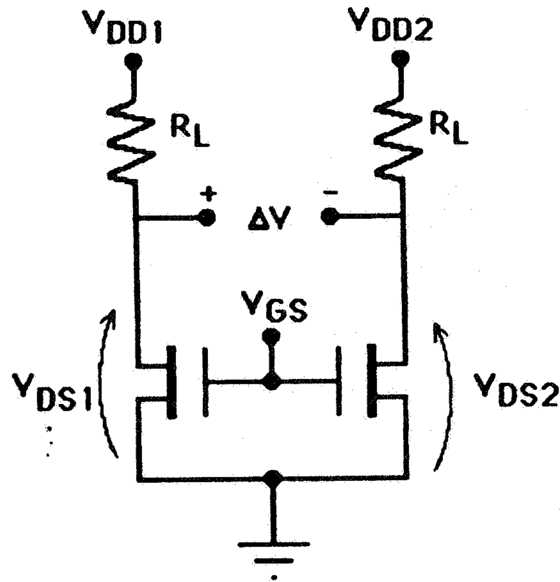

Figure 14: Measurement circuit for determination of magnetic field sensitivity.

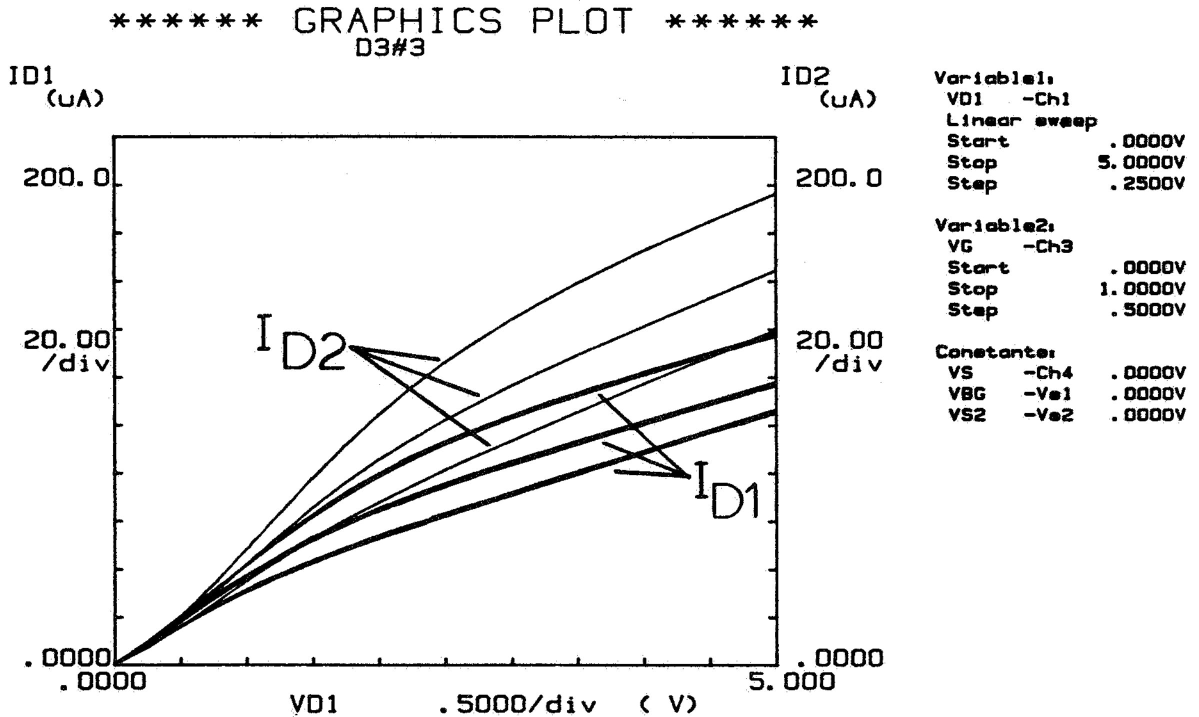

Figure 15: Measured characteristics of typical dual- drain field effect transistor.

1. Report No. NASA CR-178045	2. Government Accession No.	3. Recipient's Catalog No.
4. Title and Subtitle Advanced Detectors and Signal Processing		5. Report Date February 1986 6. Performing Organization Code
7. Author(s) D. W. Greve, P. H. L. Rasky, and M. H. Kryder		8. Performing Organization Report No.
9. Performing Organization Name and Address Dept. of Electrical and Computer Engineering Carnegie-Mellon University Pittsburg, PA 15213		10. Work Unit No. 11. Contract or Grant No. NAG1-395
12. Sponsoring Agency Name and Address National Aeronautics and Space Administration Washington, DC 20546		13. Type of Report and Period Covered Contractor Report 14. Sponsoring Agency Code 505-90-23, 506-90-23
15. Supplementary Notes Langley Technical Monitor: Paul J. Hayes Final Report - 9/1/84 - 8/31/85		

16. Abstract

Continued progress is reported toward development of a silicon- on-garnet technology which would allow fabrication of advanced detection and signal processing circuits on bubble memories. The first integrated detectors and propagation patterns have been designed and incorporated on a new mask set. In addition, annealing studies on spacer layers have been performed. Based on these studies, it is proposed that a new double layer spacer should reduce contamination of the silicon originating in the substrate. Finally, the magnetic sensitivity of uncontaminated detectors has been measured from the last lot of wafers. The measured sensitivity was lower than anticipated but still higher than present magnetoresistive detectors.

17. Key Words (Suggested by Author(s))	18. Distribution Statement
Bubble domain, MOSFET Garnet, Recrstallized silicon, Silicon-on-garnet	Unclassified-Unlimited Subject Category 33

19. Security Classif. (of this report)	20. Security Classif. (of this page)	21. No. of Pages	22. Price
Unclassified	Unclassified	27	A03

N-305

For sale by the National Technical Information Service, Springfield, Virginia 22161